Int. J. Advanced Design and Manufacturing Technology, 2022, Vol. 15, No. 4, pp. 125-132

DOI: 10.30486/admt.2023.1961907.1358 ISSN: 2252-0406 https://admt.isfahan.iau.ir

Feed Stock Fabrication of AISI 4605 Steel for Fused Deposition Modeling and Sintering and Designing of Its Extruder Mechanism

Amir Hossein Rahimi*
Department of Mechanical Engineering,
K.N. Toosi University of Technology, Iran
E-mail: Ah.Rahimi@email.kntu.ac.ir
*Corresponding author

Jamal Zamani
Department of Mechanical Engineering,
K.N. Toosi University of Technology, Iran
E-mail: Zamani@kntu.ac.ir

Received: 26 June 2022, Revised: 19 September 2022, Accepted: 25 September 2022

Abstract: Fused Deposition Modeling and Sintering (FDMS) is one of the indirect and emerging processes of Additive Manufacturing (AM) for the production of metal parts, which is a combination of AM process and Metal Injection Molding (MIM). This study laboratory made a raw material (Feed Stock) composing of high percentage of metal powder (particle in nano-scale) and polymeric materials; and then, designed an extruder to simulate melting and extruding process by Computational Fluid Dynamic (CFD). The different variables such as the nozzle diameter (D) of 1, 2, 3 and 4 mm and compression zone length (L2) of 100, 200 and 300 mm were simulated to investigate their impacts on flow rate and required torque to rotate screw. The findings showed that components of feed stock for high physical and mechanical properties of FDMS should account for 55 wt.% of paraffin wax, 25 wt.% of polypropylene, 15 wt.% of carnauba wax and 5 wt.% of stearic acid with optimum percentage of metal powder of 90 wt.%. Also, the optimum value of extruder diameter and compression zone length were 2mm and 200 mm, respectively.

Keywords: Additive Manufacturing, AISI 460 Steel Alloy, Extruder Screw, Fused Deposition Modeling and Sintering

Biographical notes: Amir Hossein Rahimi received his MSc in Material Engineering from Malek Ashtar University of Technology (MAUT) in 2008 and currently is PhD student at Department of Mechanical Engineering in K.N. Toosi University of Technology. His current research interest includes Additive Manufacturing Technology. **Jamal Zamani** is full professor of Mechanical engineering at the University of KNTU. He received his PhD in Mechanical engineering from Tarbiyat Modares University in 2003. His current research focuses on AM and FDMS.

Research paper

1 INTRODUCTION

Additive Manufacturing is a term for a class of manufacturing techniques that use the process of layer-by-layer manufacturing using computer-aided design [1]. A wide range of raw materials, such as polymeric materials with low melting temperatures to metals and ceramics with high melting point with different forms of liquid, powder and wire are used in these processes [2]. Nowadays, research in the field of additive manufacturing is no longer focused on the production of polymer prototypes and the aim of developing these techniques is to produce functional metal parts with complex shapes, which cannot be easily produced by conventional methods that have applications in the field of aerospace, automobiles, fast tools and medicine [3]. The additive manufacturing process for the manufacturing of metal parts is divided into two categories: direct and indirect processes [4].

Direct processes include selective laser sintering, selective laser melting, laser metal deposition, electron beam melting and Binder Jetting [5-9]. The base material of most of these processes is based on powder and the energy required to melt the powder is supplied through laser beam or electron beam, which is both time-based and very costly. One of the new indirect processes in the manufacture of metal parts is Fused Deposition Melting and Sintering (FDMS).

This process is one of the most cost-effective additive manufacturing processes due to the low cost of equipment, easy operation and low cost of raw materials [10]. This process has four stages of compounding of raw material, printing the desired shape (green part), debinding and sintering [11-17]. The process of printing the part in this process is the same as fused Deposition Modelling Process (FDM), except that in the FDM process, flexible filaments with fixed diameter are always used, while, the FDMS feedstock contains high percentage of powder that increases the viscosity of the melt and makes it brittle [18-21].

Therefore, the design of the extruder in FDMS system is made custom for the selected feedstock. Rheology of raw material is the most important parameter for this reason [22]. Till date, few studies have been conducted on development of raw material of the FDMS process, but due to the great similarity between this material and the raw material in MIM process, same feedstock can be used with a little change in the percentage of its components [23].

One of the most widely used binding systems in MIM is based on polypropylene and paraffin wax-based. For example, a combination of polypropylene, paraffin wax, carnauba wax and stearic acid has been successfully applied as a binder system to produce porous micron parts made of austenitic stainless steel using steel powder [24]. In addition, various types of adhesive systems such as polypropylene base, wax base and ethylene vinyl acetate (EVA) base were used for metal injection molding of parts made of L316 stainless steel with nano meter dimensions [25].

In recant years, few researches have been conducted on the rheology of two-phase material (containing metal powder and polymeric system) used for FDMS process [26-30]. In this study, the 4605-steel feedstock has been optimized for the FDMS process and an optimized screw has been designed for extrusion of the selected feedstock. Moreover, previous works have not simulated an extrusion to melt this feed stock and compress them to satisfy the purpose of AM. Therefore, CFD approach was applied to investigate various variables such as diameter and compression zone length of extruder.

2 METHOD

In this research, first, the raw material feed is selected that contains binder constituents and optimum percentage of 4605 metal powder and in the next step, the screw of the extruder of the printer is designed on the bases of rheological properties.

2.1. Feedstock Preparation

The raw materials used in the FDMS process are a combination of metal powder and adhesive system, called feedstock. This material should be injectable in the first step so that it can be injected with the help of extruder and then it should have the highest allowable powder volume so that the final piece has the lowest porosity and the highest mechanical properties. There are many parameters including the size, shape and percentage of metal powder as well as polymer components and their percentage that influences the final properties of the product in this process.

In this research, AISI 4605 low alloy steel powder (Jiangxi Yuean Superfine Metal Co., Ltd., China) produced by gas atomizing method has been produced. "Table 1" shows the chemical composition, cumulation density, D-Value values as well as distribution slope parameter (Sw) of the powder used. The slope parameter of the distribution, which indicates the slope of the powder grain size distribution and indeed the slope of the normal logarithmic cumulative distribution curve, is measured by "Eq. (1)" [22]:

$$S_w = \frac{2/56}{log\left(\frac{d90}{d10}\right)} \quad (1)$$

Table 1 The specifications of AISI 4605 steel powder in this research

Apparent Density (g/cm^3)	Slope Parameter Distribution (Sw)	Particle Size Distribution (μm)			Chemical Composition (Wt%)				
		D_{10}	D_{50}	D_{90}	Fe	C	Ni	Mo	Si
2.6	4.53	1.97	3.92	7.23	Bal.	0.42	2.15	0.49	0.1

One of the important features of the powder used in the process is the widespread distribution of powder grains of different sizes, leading to high density in the final piece and the use of less adhesive system during the process. From the point of view of particle size distribution, the powder suitable for the injection process should have a distribution slope value greater than 2 and consequently the particle size distribution should be wide. Under these conditions, higher compression density is achievable and less adhesive system is required for raw material preparation. On the other hand, powders with high sw values (more than 7) with very narrow size distributions are not suitable for the injection process [31]. According to Equation (1), the distribution slope for the powder used in this study is 4.53. Therefore, the powder used has an acceptable distribution slope which makes it suitable for use in the injection process from the nozzle with the aim of increasing the compression density of the powder and consequently the density of the sintered piece. Also, to help with the sintering, the use of powder particles with sizes between 0.1 and 20 microns and spherical shape is suitable [32], in which spherical powder with an average of particles less than 10 microns has been used. Polypropylene has also been used as a backbone polymer. This polymer, which performs the task of maintaining the shape of the piece during the adhesion process and before sintering, has been used in many researches as a suitable material as backbone polymer [33]. In the following, paraffin wax and carnauba wax have been used as surface activators in order to create a bond between adhesive system and powder grains. These materials increase the stability of powder grains due to shear stress during the mixing process. Also, carnauba wax, due to its extensive decomposition temperature, helps to preserve the shape of the piece at the time of boiling spit to the backbone polymer [33]. Stearic acid has also been added to the adhesive system as a lubricant and terrier to improve flowability and lubrication [33-34]. This compound is similar to the study of S.Ahn [35] and Lin [36], which has 55 wt.% paraffin wax, 25 wt.% polypropylene, 15 wt.% carnaoba wax and 5 wt.% staric acid as the binder system. As mentioned above, one of the most important parameters in feedstock is the percentage of metal powder, the high percentage of which increases the properties of the final piece and at the same time increases the viscosity that makes the extruding work of the material difficult and therefore should be optimized. One of the methods for calculating the optimum amount of powder is to calculate the critical volume concentration of powder or CPVC, which is determined by calculating the maximum torque during the mixing of the binder and powder system [37]. In this study, the amount of torque in terms of time for mixing feedstock in different weight percentages of powder in the range of 87-95 wt.% was investigated and the critical volume concentration of the powder was calculated.

In order to prepare the adhesive system and perform the mixing of raw materials, HAAKE Rheomix PolyLab QC Lab Mix equipped with a pair of Z-shaped blades has been used. The mixing temperature is selected based on the maximum melting temperature of the adhesive system components (polypropylene), 190°C. According to similar researches [38]. mixing speed of 75 rpm and mixing time of 20 minutes were considered. After the mixing process, the mixture was cooled to room temperature and turned into granules.

2.2. Evaluation of Feed Properties of Raw Material Produced

In order to simulate the rheology of the material and design the nozzle of the printing machine, the feed parameters of the raw material are required. For this purpose, rheological properties of prepared feeds have been calculated using torque flow and rheological tests to determine the appropriate amount of adhesive system components.

3 DESIGNS OF FDMS NOZZLE

In order to study the relations governing the internal flow geometry of the FDMS nozzle (extruder) by considering the raw material feed rheology (melt flow index and feed material viscosity index) and the screw cylinders, computational fluid dynamics (CFD) using input parameters was given to the simulation software and finally, using the input parameters of the extruder nozzle (D) and the length of the compression zone (L2), the output flow rate of the raw material and the torque were calculated to determine the power of the screw actuation motor. The work is done.

The length of the compression zone (L2) is very important considering the compression ratio (ε). In a similar study, the length of this area is less than one third of screw [20]. Also, one of the most important parameters for designing the extruder of the FDMS device is determining the output diameter of the extruder nozzle (D), which has an important effect on the resolution of the printed sample. In the present study, the effects of

compaction zone lengths (L2) and different output diameters (D) on the feedstock melting process, screw pressure distribution, velocity distribution at output, torque required for screw rotation and average output flow were investigated.

In this research, a 25 mm diameter screw with a rotational speed of R =15 rpm and a cylinder with a fixed length of L =300mm were used in which a solid feedstock with ambient temperature (25 °C) enters the cylinder funnel. Feedstock extrusion temperature of 190 °C similar to previous researches [35-36] are fixed parameters in the simulation. The space between the screw and the cylinder is meshed by the snapy Hex-Mesh tool in Open-FOAM software, for which a three-dimensional unstructured mesh with 856,251 pieces is used.

To solve the phenomenon of melting and compaction of feedstock, the rho-Pimple-Foam solvent in Open-FOAM software is used to solve the flow in three-dimensional compressibility. The Equations of continuity, momentum and governing energy in the solvent are used according to Equations (2) to (7) [37]:

$$d\rho/dt+\nabla.(\rho V)=0 \quad (2)$$

$$D(\rho V)/Dt=\nabla.\sigma \quad (3)$$

$$\sigma=-pI+\tau=-pI+\mu[(\nabla.V)+(\nabla.V)^{T}]-2\mu/3\ (\nabla.V)I \quad (4)$$

$$D(\rho e)/Dt+\nabla.(\rho VV+pI)=\nabla.(k\nabla T)+\mu\Phi \quad (5)$$

$$e=1/2\ V^{2}+u \quad (6)$$

$$\Phi=\tau:\nabla V \quad (7)$$

Where, v, p, e, u and I represent the velocity, pressure, total energy, internal energy and matrix vectors, respectively. The parameters ρ, μ, and k also indicate density, viscosity, and heat transfer coefficient, respectively. In the momentum relation, the stress component (σ) consists of compressive, shear (τ) stresses and element volume changes. Also in the energy Equation, the effects of volume change and heat loss (Φ) due to viscosity are considered. Parameter (e) is also the sum of the kinetic and internal energy of the fluid. Shear stress on the extruder wall (τ), torque (T) and output flow (m □_o) are calculated using the following Equations:

$$\tau = \mu \frac{\partial U}{\partial n} \text{ on screw wall} \quad (8)$$

$$T = \iint r\,\tau\,dA\,dz \quad (9)$$

$$\dot{m}_o = \int \rho U dA \quad (10)$$

In Eq. (9), r, τ, dA represent the cross-sectional area of the element, the shear stress on the element and the distance of the element from the center of the rotating axis, respectively. The boundary conditions used in the simulation include the following:

- Boundary conditions at the aperture entrance:
  Material feed, or in other words, the inlet velocity is regulated by suction rotation and the inlet temperature of the material is assumed to be environmental 25℃.
- Boundary conditions at the orifice output:
  The output speed and temperature are adjusted according to the screw speed and the feedstock melt temperature.
- Cylinder inner wall boundary conditions:
  The velocity of the fluid inside the cylinder is a function of screw's rotational speed. For this purpose, a rotating axis is provided for it. Its rotation speed is 15rpm and its temperature is 190℃.

4 RESULTS

4.1. CPVC

Torque values versus the time for feed mixing for different weight percentages of powder (87-95 wt.%) are shown in "Fig. 1a". As can be seen in the figure, the average torque values increase linearly with increasing weight percentage of powder till 92 wt.%. This increase continues until the slope of the line changes abruptly due to the lack of binder, which is accompanied by an increase in friction between the excess amount of powder grains in the feed. Figure 1.b also shows the mean mixing torque values in different weight percentages of powder in the feed, which is plotted by passing a line through the average values for each weight percentage of powder in the feedstock.

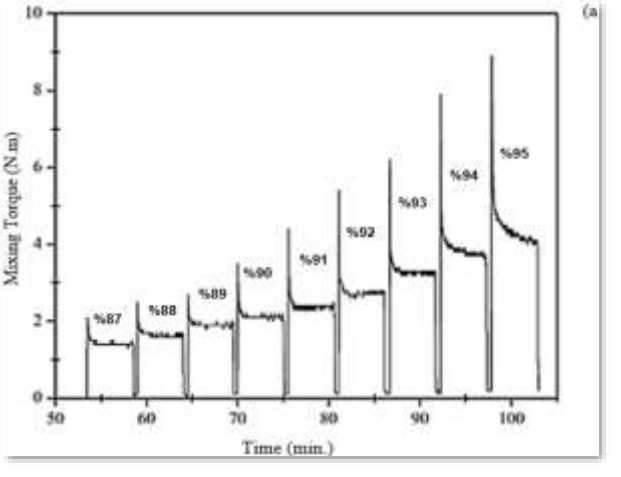

a

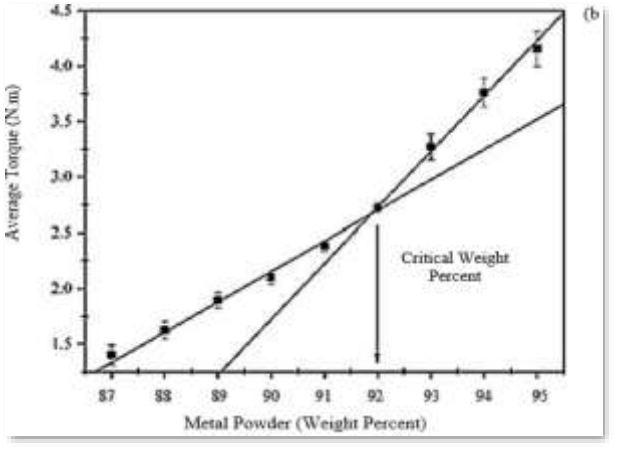

b

Fig. 1 The powder critical weight measurement: (a): mixing torque versus time at different powder weigh percentages, and (b): average torque at different powder weigh percent.

When the slope of the line begins to change, it means reaching the critical weight percentage of the powder. Finally, in order to increase the flowability and prevent instability of the rheological properties of the optimal powder content in the feedstock, it is usually considered to be 2 to 5% lower than the critical powder content in the feedstock [38], The weight content of the powder in the feed of the raw material is considered to be 90% by weight.

4.2. Viscosity

The results of rheological tests and how the viscosity logarithm changes according to the logarithm of the shear rate for the optimal adhesive system at 190 are shown in "Fig. 2".

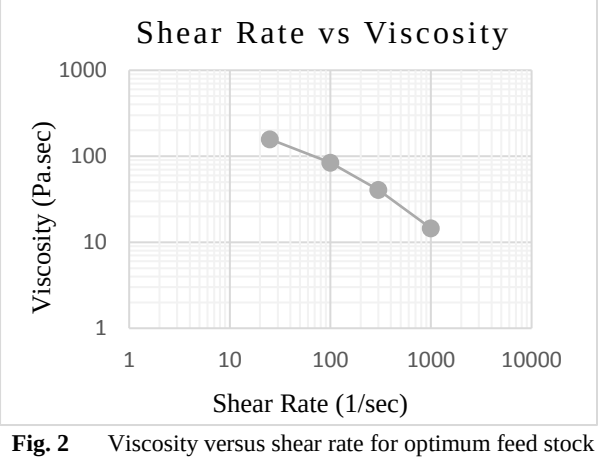

Fig. 2 Viscosity versus shear rate for optimum feed stock at different temperatures.

Sotomayor et al. [39] estimated the viscosity values for a successful injection molding (MIM) process to be less than 1000 Pa.s in the cut-off range between S-1100 to S-1 10,000. Therefore, from a rheological point of view, the results show that the feed can be injected in this interval.

4.3. Simulation Results

Figure 3a shows the effects of changes L2 and D on the torque required to extrude the raw material. As can be seen in the Figure, with increasing L2, first the torque decreases due to gradual melting and compaction of the melt, and then after L2 = 200 mm, it increases due to the enlargement of the compression zone and the melting zone. Increasing L2 leads to gradual compression of the raw material, which reduces the shear stress in the melt and increases the shear stress between the screw and the cylinder wall.

It can also be seen in "Fig. 3" that the torque decreases with increasing material flow and decreasing type I stress. The reason for the increase in torque at D = 1mm is that in a very small diameter of the nozzle, the stress of the first type is much higher than the second type. Figure 3b shows the effects of L2 and D on the output flow rate of the raw material.

As can be seen, with increasing L2, the output flow increases due to the gradual increase in pressure inside the extruder. An increase in D also indicates an increase in the flow rate. The reason for the sudden drop in flow velocity at D = 1 compared to other cylinder diameters is the presence of metal powder, which results in a high viscosity of the melt that must pass through a very small diameter of 1 mm.

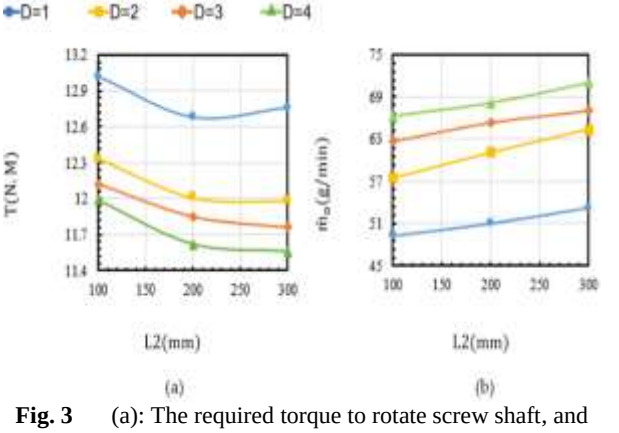

Fig. 3 (a): The required torque to rotate screw shaft, and (b): output flow rate ($\dot{m}_o$).

In "Fig. 4", the melting process is visible along the extruder for D = 2mm, in which blue represents the solid phase and red represents the liquid phase. In all cases it can be said that the feedstock melts at less than the first 0.25 L of screw. It is also observed that the increase in L2 has little effect on the melting zone.

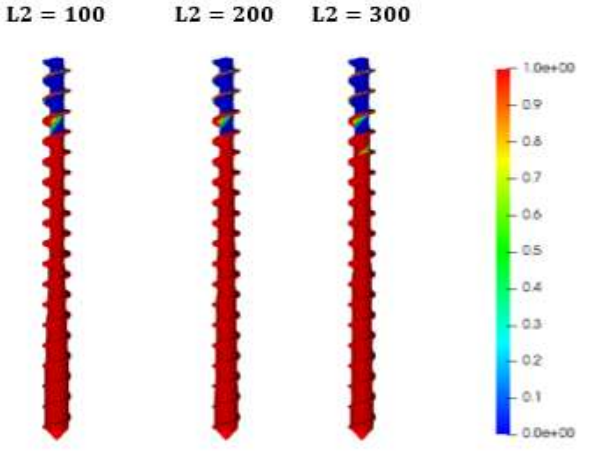

Fig. 4 Melting process along extruder for various L2 at D=2 mm.

Figure 5 shows the temperature distribution on the extruder at different diameters of the extruder cylinder. As can be seen, an increase in D increases the output flow, which in turn requires more heat to melt the raw material.

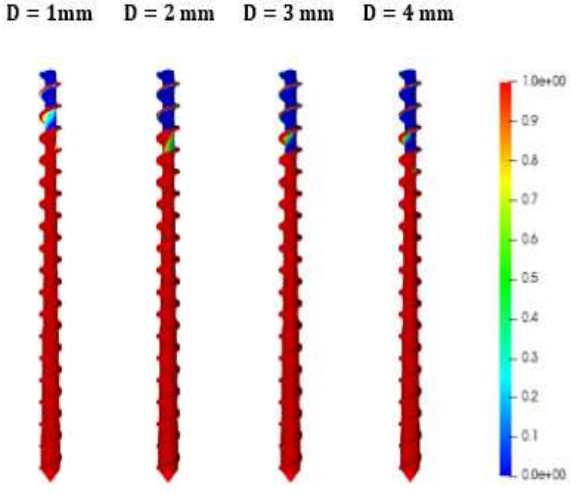

Fig. 5 Melting process along extruder for various D at L2=200 mm.

Figure 6 shows the pressure distribution on screw for different L2 values at D = 2mm and "Fig. 7" shows the pressure distribution on screw for different nozzle diameters at L2 = 200mm. All inlet pressure is atmospheric pressure, which increases to 0.75 L by moving along the screw axis and then decreases due to the discharge of melt out of the cylinder. It can also be seen that increasing L2 due to uniform compression of the melt reduces the maximum pressure and with increasing D the pressure inside the screw cylinder decreases and moves upwards of the extruder.

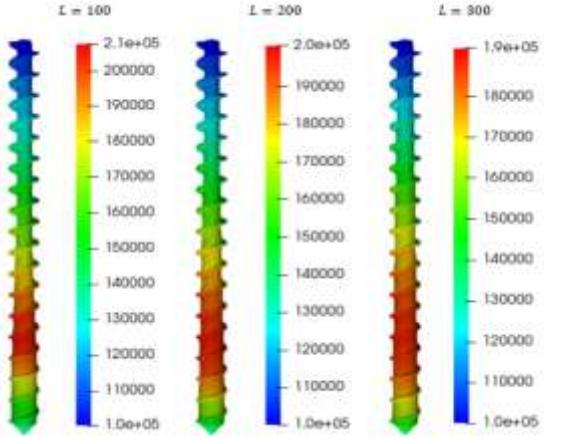

Fig. 6 Pressure distribution on screw shaft for various L2 at D=2 mm.

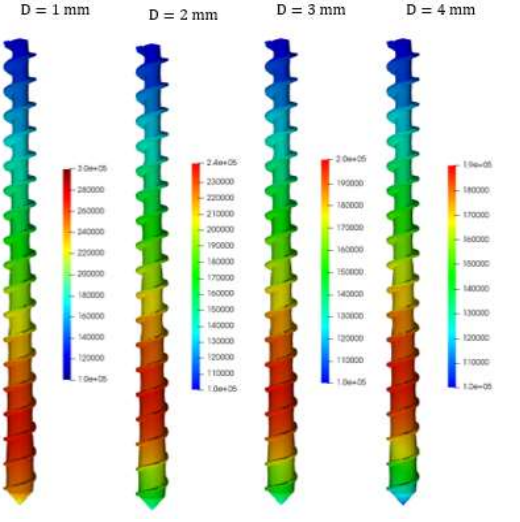

Fig. 7 Pressure distribution on screw shaft for various D at L2=200 mm.

The output velocity distribution for the extruder design and the flow rate distribution of the printed material in "Figs. 8 and 9" for different L2s at D = 2mm and different nozzle diameters at L2 = 200mm, are shown respectively. In all cases, the maximum velocity occurs in the center and near the nozzle walls. The results show that increasing L2 leads to increasing the maximum speed and increasing D leads to decreasing the maximum speed at the output.

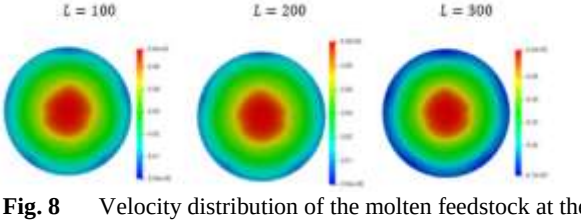

Fig. 8 Velocity distribution of the molten feedstock at the output for various L2 at D=2 mm.

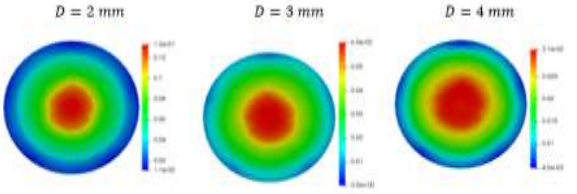

Fig. 9 Velocity distribution of the molten feedstock at the output for various D at L2=200 mm.

Figure 10a shows that by increasing L2, the maximum pressure inside the cylinder decreases. This causes the raw material to gradually thicken. On the other hand, increasing D makes it easier to extrude the molten raw materials in the extruder and reduces the maximum pressure. Figure 10b shows the maximum speed at the extruder output. As can be seen, the maximum velocity increases linearly with increasing L2. The output velocity can also be inversely related to D because the rotational speed of the screw axis is constant, so that increasing D reduces the velocity of the molten raw material. The reason for the decrease in extrusion speed with diameter D = 1 compared to diameter D = 2 can be related to the high viscosity of the feed melt and the high percentage of metal powder inside the raw material, which causes problems during the extrusion process at low diameters.

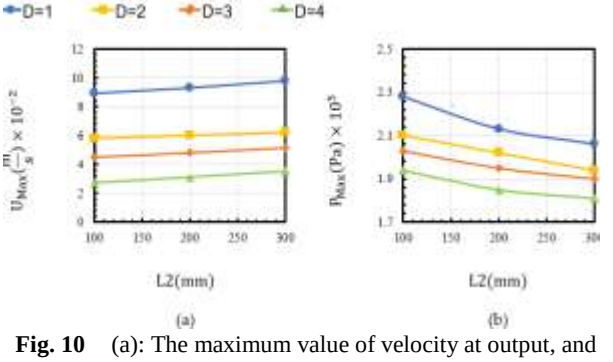

Fig. 10 (a): The maximum value of velocity at output, and (b): the maximum value of pressure inside extruder.

5 CONCLUSIONS

In this study, an binder system similar to that of S.Ahn and Kuang-hon Lin [35-36] containing 55 wt. % Paraffin wax, 25% polypropylene, 15% carnauba wax, and 5 wt. % Stearic acid was used according to the similarity of the powder used and the percentage of 4605 powder used was calculated using CPVC method equal to 90% by weight. Then, by extracting the rheological properties of the raw material, the extruder of the FDMS device has been designed. The effect of different compression lengths (L2) and extruder nozzle diameter (D) on melt temperature, pressure, outlet velocity and initial flow velocity were also investigated. In this study it was shown that the melt output from the nozzle D = 1mm was less than D = 2mm. This may be due to the higher melt stresses between the screw and the cylinder in the smaller nozzles. Also, it was shown that L2 = 200 mm leads to a softer melt with lower extrusion torque. Finally, it was found that the optimal design of the extruder with D = 2 and L2 = 200 mm with the required torque of 12N.M and the output melt flow of about 64 gr/min is a suitable design for the extruded feed 4605 made in this research.

REFERENCES

[1] ASTM Standard, F2792, Standard Terminology for Additive Manufacturing Technologies, ASTM International, West Conshohocken, Pennsylvania, 2012.

[2] West, A. P., Sambu, S. P., and Rosen, D. W., A Process Planning Method for Improving Build Performance in Stereolithography, Computer Aided Design, 2001, pp. 65–79.

[3] Li, N., Huang, S., Zhang, G., Qin, R., Liu, W., Xiong, H., Shi, G., and Blackburn, J., Progress in Additive Manufacturing on New Materials: A Review, J. Mater. Sci. Technol., Vol. 35, No. 2, 2019, pp. 242–269.

[4] Rahimi, A. H., Zamani, J., Development of a Feedstock for Additive Manufacturing of 4605 Steel Compact by FDMS Process, Transactions of the Indian Institute of Metals, 2022, pp. 1-7.

[5] Agarwala, M., Bourell, D., and Beaman, J., Direct Selective Laser Sintering of Metals, Rapid Prototyping, No. 1, 1995, pp. 26–36.

[6] Aghanajafi, C., Daneshmand, S., and Nadooshan, A. A., Influence of Layer Thickness on The Design of Rapid-Prototyped Models, Journal of aircraft, Vol. 46, No. 3, 2009, pp. 981-987.

[7] Korinko, P. S., Adams, T. M., Malene, S. H., Gill, D., and Smugeresky, J., Laser Engineered Net Shaping for Repair and Hydrogen Compatibility, Weld. J., Vol. 90, No. 9, 2011.

[8] Daneshmand, S., Ahmadi, A., and Aghanajafi, C., Design and Production of Wind Tunnel Testing Models with FDM Technology Using ABSi, International Journal of Manufacturing Research, Vol. 4, No. 2, 2009, pp. 120-136.

[9] Do, T., Seop Shin, Ch., Stetsko, D., VanConant, G., Vartanian, A., Pei, Sh., and Kwon, P., Improving Structural Integrity with Boron-Based Additives for 3D Printed 420 Stainless Steel, Procedia Manuf., Vol. 1, 2015, pp. 263–272.

[10] Rane, K., Strano, M., A Comprehensive Review of Extrusion-Based Additive Manufacturing Processes for Rapid Production of Metallic and Ceramic Parts, Adv. Manuf, Vol. 7, No. 2, 2019, pp. 155–173.

[11] Agarwala, M. K., Jamalabad, V. R., Langrana, N. A., Safari, A., Whalen Ph. J., and Danforth, S. C., Structural Quality of Parts Processed by Fused Deposition, Rapid Prototyp. J., Vol. 2, No. 4, 1996, pp. 4–19.

[12] Momeni, V., Hossein Alaei, M., Askari, A., Hossein Rahimi, A., and Nekouee, K., 2019. Effect of Carnauba Wax as A Part of Feedstock on The Mechanical Behavior

of a Part Made Of 4605 Low Alloy Steel Powder Using Metal Injection Molding, Material Wissen chaft und Werk Stoff Technik, Vol. 50, No. 4, 2019, pp. 432-441.

[13] Bin L., Yuxiang, W., Ziwei, L., and Tao, Zh., Creating Metal Parts by Fused Deposition Modeling and Sintering, Mater. Lett. 18, Vol. 263, 2020.

[14] Rahimnia, A., Hesarikia, H., Rahimi, A., Karami, S. and Kaviani, K., Evaluation and Comparison of Synthesised Hydroxyapatite in Bone Regeneration: as an in Vivo Study, Journal of Taibah University Medical Sciences, Vol. 16, No. 6, 2021, pp. 878-886.

[15] Tarafdar, A., Razmkhah, O., Ahmadi, H., Liaghat, G., Chitsaz Charandabi, S., and Rezaei Faraz, M., Effect of Layering Layout on The Energy Absorbance of Bamboo-Inspired Tubular Composites, Journal of Reinforced Plastics and Composites, 2022, pp. 07316844211063865.

[16] Agarwala, M. K., Van Weeren, R., Vaidyanathan, R., Carrasquillo, G., Jamalabad, V., Langrana, N., Safari, A., Garofalini, S. H., and Danforth, S. C., Structural Ceramics by Fused Deposition of Ceramics, Vol. 6, 1995. pp. 1–8.

[17] Agarwala, M. K., Van Weeren, R., Bandyopadhyay, A., Whalen, P. J., Safari and A., Danforth, S. C., Fused Deposition of Ceramics and Metals: An Overview, Proc. Solid Free. Fabr. Symp., 1996, pp. 385–392.

[18] Yang, X., Xie, H., He, Q., Zhou, Z., Xu, X., Zhang, L., and Xie, Z., Study of Thermal Degradation of Binders for Ceramic Injection Melding by TGA-FTIR, Ceram. Int, Vol. 45, No. 8, 2019, pp. 10707–10717.

[19] Momeni, V., Askari, A., Alaei, M.H., Rahimi, A.H., Nekouee, K., and Zangi, H., The Effect of Powder Loading and Binder System on The Mechanical, Rheological and Microstructural Properties Of 4605 Powder in MIM Process, Transactions of the Indian Institute of Metals, Vol. 72, No. 5, 2019, pp. 1245-1254.

[20] He, Q., Jiang, J., Yang, X., Zhang, L., Zhou, Zh., Zhong, Y., and Shen, Zh., Additive Manufacturing of Dense Zirconia Ceramics by Fused Deposition Modelling Via Screw Extrusion, Journal of the European Ceramic Society, Vol. 41, 2021, pp. 1033–1040.

[21] Boparai, K. S., Singh, R., and Singh, H., Development of Rapid Tooling Using Fused Deposition Modelling: A Review, Rapid Prototyping Journal, Vol. 22, No. 2, 2016, pp. 281–299.

[22] Huang, B., Liang, S., and Qu, X., The Rheology of Metal Injection Melding, J. Mater. Process. Technol., Vol. 137, No. 1, 2003, pp. 132–137.

[23] Gülsoy, H. Ö., German, R. M., Production of Micro-Porous Austenitic Stainless Steel by Powder Injection Molding, Scr. Mater., Vol. 58, No. 4, 2008, pp. 295–298.

[24] Supriadi, S., Baek, E. R., Choi, C. J., and Lee, B. T., Binder System for STS 316 Nano-Powder Feedstocks in Micro-Metal Injection Molding, J. Mater. Process. Technol., Vol. 187–188, 2007, pp. 270–273.

[25] Onbattuvelli, V. P., Enneti, R. K., Park, S. J., and Atre, S. V., The Effects of Nanoparticle Addition on SiC and AlN Powder-Polymer Mixtures: Packing and Flow Behavior, Int. J. Refract. Met. Hard Mater., Vol. 36, 2013, pp. 183–190.

[26] Bellini, A., Bertoldi, M., Liquefier Dynamics in Fused Deposition Modelling, Journal of Manufacturing Science and Engineering, Vol. 126, 2004, pp. 237-246.

[27] Sa'ude, N., Ibrahim, M., and Ibrahim, M. H. I., Melt Flow Behavior of Polymer Matrix Extrusion for Fused Deposition Modeling (FDM), Vol. 660, 2014, pp. 89–93, AMM.

[28] Cobos, C. M., Garzón, L., López Martinez, J., Fenollar, O., and Ferrandiz, S., Study of Thermal and Rheological Properties of PLA Loaded with Carbon and Halloysite Nanotubes for Additive Manufacturing, Rapid Prototyping Journal, Vol. 25 No. 4, 2019, pp. 738-743.

[29] Ramanath, H. S., Chua, C. K., and Leong, K. F., Melt Flow Behaviour of Poly-I Caprolactone in Fused Deposition Modelling, Journal of Material Science, Materials in Medicine, Vol. 19, No. 7, 2007, pp. 2541-2550.

[30] Nikzad, M., Masood, S. H., Sbarski, I., and Groth, A., Thermo-Mechanical Properties of a Metal-Filled Polymer Composite for Fused Deposition Modelling Applications, In: Proceedings of 5th Australasian Congress on Applied Mechanics, Brisbane, Australia: Australian Congress on Applied Mechanics, 2007.

[31] Sotomayor, M. E., Várez, A., and Levenfeld, B., Influence of Powder Particle Size Distribution on Rheological Properties of 316L Powder Injection Moulding Feedstocks, Powder Technol., Vol. 200, No. 1–2, 2010, pp. 30–36.

[32] Atre, S. V., Weaver, T. J., and German, R. M., Injection Molding of Metals and Ceramics, Metal Powder Industries Federation, 1998.

[33] Ho, Y. L., Lin, S. T., Debinding Variables Affecting the Residual Carbon Content of Injection-Molded Fe-2 Pct Ni steels, Metall. Mater. Trans. A, Vol. 26, No. 1, 1995, pp. 133–142.

[34] Matsuda, M., Miura, H., Mechanical Properties of Injection Molded Fe-6% Ni-0.4% C Steels with Varying Mo Contents of 0.5 to 2%, Met. Mater. Int., Vol. 9, No. 6, 2003, pp. 537–542.

[35] Ahn, S., Park, S. J., Lee, S., Atre, S. V., and German, R. M., Effect of Powders and Binders on Material Properties and Melding Parameters in Iron and Stainless-Steel Powder Injection Melding Process, Powder Technology, Vol. 193, 2009, pp. 162-169.

[36] Lin, K., Wear Behavior and Mechanical Performance of Metal Injection Molded Fe–2Ni Sintered Components, Mater. Des., Vol. 32, No. 3, 2011, pp. 1273–1282.

[37] Klainerman, S., Majda, A., CompressibL2e and IncompressibL2e fL2uids, Communications in Pure AppL2ied Mathematics, Vol. 35, 1982, pp.629-651.

[38] German, R. M., Bose, A., Injection Molding of Metals and Ceramics, Metal Powder Industries Federation, 1997.

[39] Sotomayor, M. E., Levenfeld, B., and Várez, A., Powder Injection Moulding of Premixed Ferritic and Austenitic Stainless-Steel Powders, Mater. Sci. Eng. A, Vol. 528, No. 9, 2011, pp. 3480–3488.